Effect of an upstream tall building on a street canyon flow

Haoran Du, Eric Savory, L. Perret

PHYSMOD 2022 – International Workshop on Physical Modeling of Flow and Dispersion Phenomena
Institute of Thermomechanics of the CAS, Prague, Czech Republic – August 29-31, 2022

Effect of an upstream tall building on a street canyon flow

Haoran Du[1], Eric Savory[1], Laurent Perret[2]

[1]University of Western Ontario, Department of Mechanical and Materials Engineering, 1151 Richmond Street, N6A 3K7 London, Canada
[2]Nantes Université, École Centrale Nantes, CNRS, LHEEA, UMR 6598, F-44000 Nantes, France

Abstract

The wake effect caused by high-rise buildings could have a strong influence on the boundary layer and result in a strong impact on the turbulence associated with street canyon flows. A wind tunnel experiment was performed to investigate this, focusing on a realistic street canyon configuration embedded in a realistic urban fabric. A morphographic scale model of the centre of Nantes, France, at the scale of 1:200 was used, in which the Rue de Strasbourg was the investigated canyon and the nearby cathedral was identified as the local tall building. To complement this investigation, additional experiments were performed by replacing the cathedral with a block building as a comparison. Stereoscopic PIV was set up to capture the vertical plane at the centre of the street canyon for turbulence statistics. The wake caused by the cathedral affects all the flow statistics, such as the mean velocities, the Reynolds stresses, and the velocity skewnesses within the shear layer. The cathedral wake was also found to reduce the vertical exchanges at roof level. Finally, strong spanwise velocities at the pedestrian level were also observed, as a result of the complex morphology of the surrounding building layout and the presence of nearby intersections.

Introduction

With the growth of the global economy, the number of designs and constructions of tall buildings in the coming years has increased progressively. A single tall building or a cluster of tall buildings within a low-rise neighbourhood could bring multiple unexpected influences on urban climates, such as strong gusts at the pedestrian level (Tominaga & Shirzadi, 2021), poor pollutant dispersion and ventilation in street canyons (Yuan et al., 2014).

Previous *in-situ*, experimental, or computational studies of urban boundary layers and street canyons focused on flow turbulence, or pollutant dispersion using idealized homogeneous roughness elements such as bars or cubes (Bottema, 1996; Inagaki & Kanda, 2008; Salizzoni et al., 2011; Blackman et al., 2015; Basley et al., 2019; Jaroslawski et al., 2019). Basley et al. (2019) stated that the flow characteristics in the inertial layer, such as coherent structures and vortices, show independence from the wall configuration, in agreement with the smooth-wall situation (Castro et al., 2013; Squire et al., 2016) and the roughness sublayer could be penetrated by large-scale motions of the overlaying boundary layer if the packing density, which is defined by the ratio of the plan area of the obstacles to the total plan area, is below a certain threshold. Some studies used idealized heterogeneous roughness such as bars and cubes whose heights followed a normal distribution (Cheng & Castro, 2002; Goulart et al., 2019) or examined different element spacings (Choi et al., 2020; Cheng et al., 2021), or focused on the effects of the different roof shapes (Schultz et al., 2007) and orientation of the buildings in roughness (Yang & Meneveau, 2016). Although Cheng & Castro (2002) found that the upper limit of the inertial sublayer over a homogeneous roughness arrangement is almost identical to that over inhomogeneous roughness, while the roughness sublayer is much thinner and the friction velocity and roughness length are significantly smaller for

the latter case, studies of heterogenous simplified arrays seldom focused on the influence on the downstream boundary layer (Cheng et al., 2021).

Furthermore, tall buildings, in accordance with their definition, are extreme outliers to the height distribution of the upstream roughness and, hence, cannot simply be represented by the normal distribution. Tall buildings protrude across the roughness sublayer which extends two or three times the mean building height above the underlying roughness (Cheng & Castro, 2002). Karman vortices, horseshoe vortices, and tip vortices are generated around and downstream of a wall-mounted finite cylinder with a high aspect ratio $AR_w = h_{cylinder}/d_{cylinder}$ (Roh & Park, 2003), and can noticeably influence the downstream boundary layer over the relatively low-height surrounding roughness. The effects of tall buildings have been, therefore, studied either in idealized roughness arrays (Brixey et al., 2009; Heist et al., 2009; Fuka et al., 2018) or morphological models (Rotach et al., 2005; Ng et al., 2011; Salizzoni et al., 2011b; Cheng et al., 2021; Hertwig et al., 2019, 2021). Cheng et al. (2021) divided the urban roughness sublayer into two layers and found that the upper layer, which is governed by tall buildings, has larger dispersive stress and smaller drag than the lower layer which contains more dense and shorter buildings. The incoming flow, influenced by the upstream low-rise canopy, strikes the tall building to generate a rooftop shear layer and the tall building's wake changes the near-wake dynamics by interacting with the downstream low-rise canopy (Lim et al., 2022). The wake caused by a tall building, therefore, could have a strong and long-distance effect on the flow and scalar field of the low-rise surrounding urban terrain and the downstream urban boundary layer (Hertwig et al., 2021).

Grimmond & Oke (1999) suggested categorizing street canyon flows into three different regimes; isolated, wake interference, and skimming, based on the building plan area density and showed that the canyon aspect ratio $AR_c = w_{canyon}/h_{canyon}$ has a large influence on street canyon flow. Studies have examined the effect of varying the geometry (2D or 3D) of the roughness elements on the boundary layer flow (Michioka & Sato, 2012; Takimoto et al., 2013) and have found that the friction velocity and shear stress increase from 2D to 3D configurations throughout the boundary layer. More detailed studies regarding both 2D and 3D arrays falling within both the skimming flow regime and the wake interference regime were studied by Blackman et al. (2015) and Jaroslawski et al. (2019), who found that the mean streamwise velocity is higher in skimming flow regime than in the wake interference regime, whilst the 2D configurations of upstream roughness yield a larger streamwise velocity than in 3D with same plan area density λ_p. They also suggested that a higher level of vertical ventilation at the roof level and larger shear stresses appear with a higher AR_c.

The same test model of the Rue de Strasbourg in Nantes, was studied in a series of experiments, either *in-situ* (Mestayer et al., 1999; Berkowicz et al., 2002; Louka et al., 2002; Vachon et al., 2002) or in wind tunnels (Kastner-Klein et al., 2004; Kastner-Klein & Rotach, 2004) to understand the turbulence and pollutant dispersion mechanism within and above the canyon considering different factors. The thermal effects caused by solar heating (Mestayer et al., 1999; Louka et al., 2002) provided insights into their influence on the pollutant concentration and wind turbulence within the street canyon and were compared with a Reynolds Averaged Navier Stokes (RANS) model that incorporated a k-ε turbulence closure named CHENSI (Sini et al., 1996). The CHENSI simulations showed two counter-rotating vortices and a small eddy at the bottom of the leeward wall which was thought to be an overestimation in comparison with the field experiment, probably due to the potential error in its wall function and the limitation of the 2D simulation. The traffic-induced

turbulence and pollutant dispersion were studied (Berkowicz et al., 2002; Vachon et al., 2002) in comparison with the Danish Operational Street Pollution Model (OSPM) (Berkowicz, 2000) and Micro Scale Air Pollution Model (MISKAM) (Eichhorn, 1996). The dependence of pollutants concentration on the wind speed was found to be less obvious on the leeward side and MISKAM was shown to be in better agreement with the field experiment than the OSPM model by considering the initial mixing of vehicle exhausting at a lower height of 2 m. The wind tunnel experiments (Kastner-Klein et al., 2004; Kastner-Klein & Rotach, 2004) used the same morphographic model as this present research while measuring with Laser Doppler Velocimetry (LDA) and placing the cathedral downstream of the street canyon. Mean streamwise velocities and shear stresses were fitted within the overlying boundary layer through parameterization of length scales and friction velocities.

All these studies focusing on the effect of upstream roughness and boundary layer on the street canyon used homogeneous arrays while, as illustrated above, the rarely investigated heterogeneous terrain and, especially, the presence of a tall building would noticeably change the boundary layer characteristics and, therefore, would strongly influence the flow and scalar field of street canyons. However, such a topic lacks abundant studies and so this aspect is the focus of the present paper.

Experiment details

The experiments were conducted in the open circuit atmospheric boundary layer wind tunnel in the LHEEA at Ecole Centrale de Nantes, which has test section dimensions of 24 m (length) × 2 m (width) × 2 m (height) and a 5:1 ratio inlet contraction. To initiate the boundary layer, five vertical tapered spires of 800 mm in height and 134 mm in width were located at the intersection of the end of the contraction and the test section, followed by a 200 mm high solid fence across the working section downstream of the inlet and then a 19 m fetch of staggered cube roughness elements with height h_1 = 50 mm and a plan area density λ_{p1} = 25 %. A 1:200 scaled morphographic model part of the city of Nantes, France, centred around the rue de Strasbourg, in which the cathedral was identified as the local tall building was placed downstream of the cubic array. The model has an upstream plan area density λ_{p2} = 44 % and an overall average ridge height of approximately 100 mm (Petra Kastner-Klein & Rotach, 2004). In another experiment, the cathedral was replaced by a 200 mm × 200mm × 100mm rectangular block, named as 1-block configuration for comparison purposes. The width of the street canyon is 73 mm, and the upstream building ridge height h_2 equals 116 mm while the downstream ridge height is 114.5 mm. The distinction between the height of the upstream roughness and the street canyon is due to the different terrain categories of suburban areas and city centre.

A Dantec particle image velocimetry (PIV) system was utilized to measure the 3-component velocity field in the vertical plane at the centre of the street canyon. LaVision Laskin-Nozzle aerosol generator was used to seed the flow with olive oil aerosol with a mean droplet diameter of 1 um. A Litron double cavity Nd-YAG laser (2 × 200 mJ) was mounted on the ceiling of the wind tunnel to generate a laser light sheet. Two 2048 x 2048 CCD cameras with 105 mm objective lenses were installed under the wind tunnel floor and used for stereoscopic PIV to record pairs of images at a frequency of 7.4 Hz between pairs of pulses and a time-step of 300 μs between two images of the same pair, as shown in Fig.1. The synchronization of the cameras and laser was controlled using Dantec Dynamic Studio software, which was also used to perform the PIV analysis on the recorded images. 10,000 pairs of images were recorded for each flow configuration and the multi-pass cross-correlation PIV processing resulted in a final interrogation window size of 32 × 32 pixels with an overlap of 50 %. For

all the configurations, the final spatial resolution was 1.6 and 3.2 mm in the longitudinal and vertical directions, respectively.

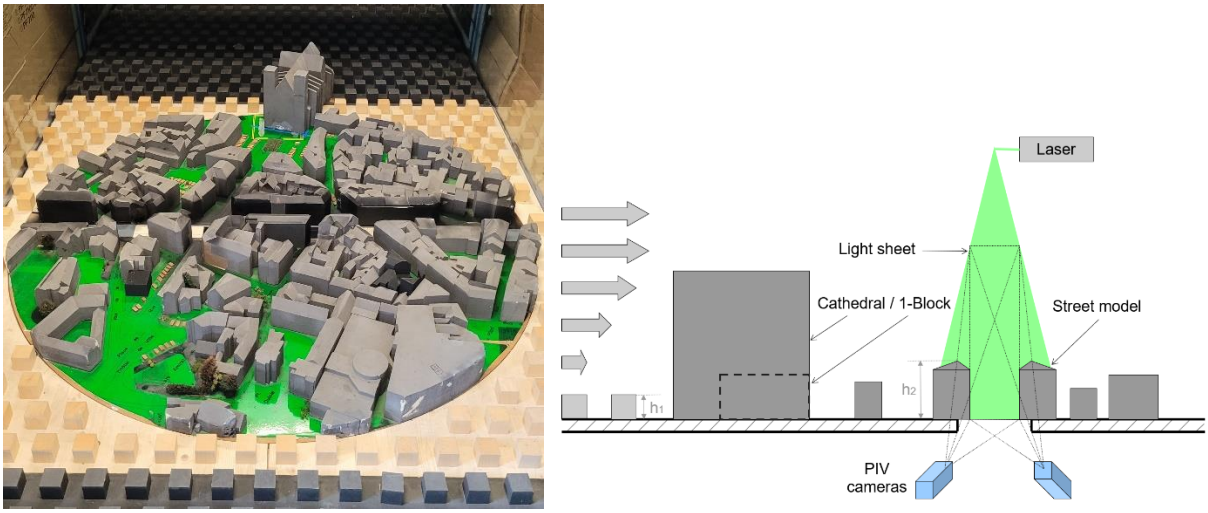

Fig 1. Left: The morphological model in the wind tunnel; Right: Stereoscopic PIV set-up

All the experiments were performed with the same free-stream velocity of U_e = 5.8 m s^{-1} measured with a pitot-static tube located 1.5 m above the wind tunnel floor and the centreline of the tunnel in the test section, without the model. The Reynolds number, based on upstream roughness height, of $Re_{h_1}=\frac{h_1 u_*}{\nu}=1.2\times10^3$ was computed and the oncoming boundary layer parameters and scaling factors are shown in Table 1.

Table 1. Oncoming boundary layer characteristics (Blackman et al., 2018)

	U_e (m s^{-1})	u_*/U_e	h_1 (m)	δ (m)	$Re_{h_1}(u_*)$	$Re_\delta(u_*)$	d/h_1	z_0/h_1	$\frac{\partial P}{\partial x}$ (Pa m^{-1})
Cathedral / 1-block	5.8	0.07	0.05	0.975	1.2×10^3	2.4×10^4	0.64	0.08	- 0.37

Results

Contours of temporally averaged components are presented below for a comparison between the scenario with the cathedral or with the replaced block in the upstream direction. Fig. 2 shows the magnitude of streamwise, vertical, and longitudinal velocity distributions by sequence. The streamwise velocity component over the canyon is noticeably smaller if the cathedral is upstream which could be explained by the fact that the induced wake downstream the cathedral is more turbulent than the overlying boundary layer flow for the 1-block configuration. This could also be observed in the vertical velocity component contour since the zone at z/h_2 = 2 shows larger magnitudes than the surroundings, which indicates some lifting effects in the observed region. In the near-wall region, the vertical component shows a general pattern, such that the most negative region is near the downstream wall and the most positive region is near the upstream wall, while the magnitude of the latter is larger than the former. Spanwise velocities were usually regarded as negligible in long symmetrical street canyon models, while a strong spanwise effect was observed at the upstream lower corner within the canyon in this presenting morphological model. This might

primarily be induced by the intersections that separated the street canyon into multiple short sections and partly be caused by the asymmetric wake generated by the upstream building since it is not situated perpendicular to the street canyon but at an angle of around 20° to the streamwise direction.

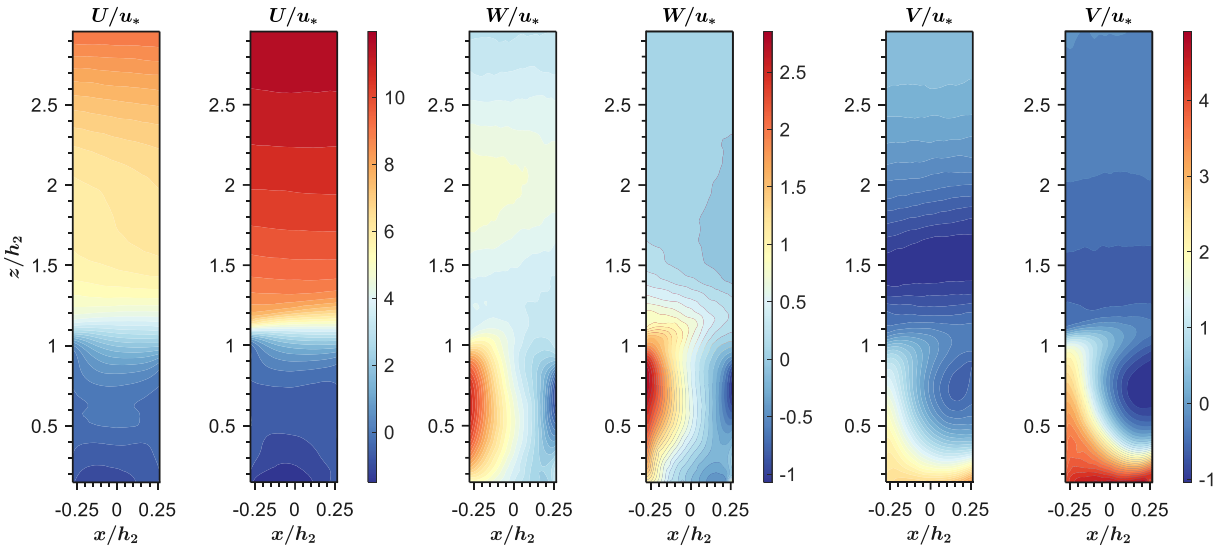

Fig 2. Comparison of contours of velocity components (Left: cathedral; Right: 1-block)

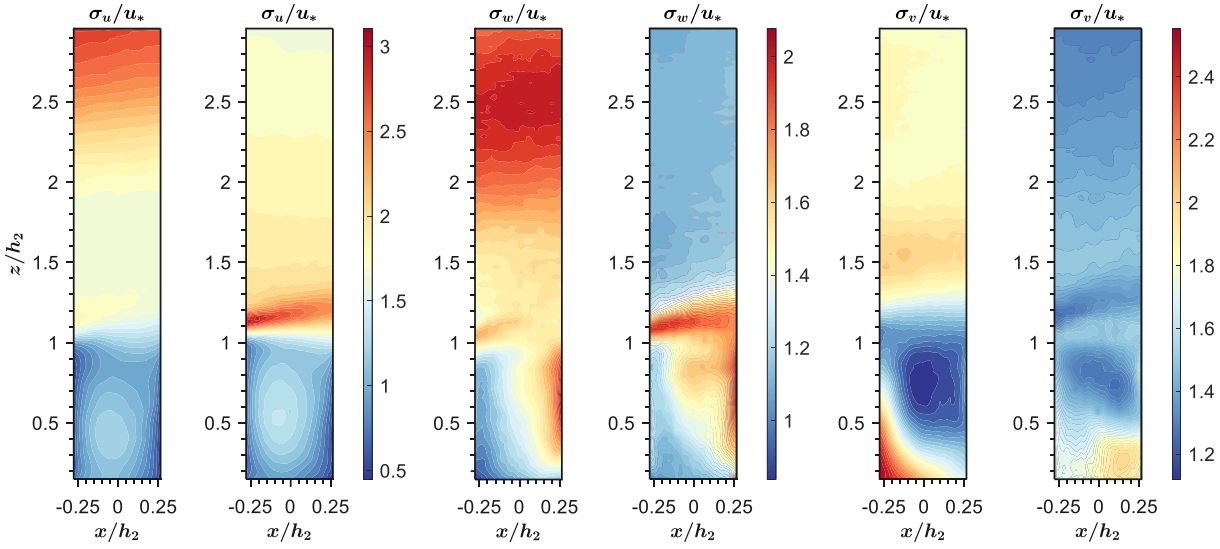

Fig 3. Comparison of contours of velocity standard deviations (Left: cathedral; Right: 1-block)

As shown in Fig 3. for the case of the cathedral, the standard deviations of velocity components in the overlying boundary layer are clearly larger while those within the shear layer are visibly smaller for the 1-block configuration. This could be explained by the wake induced by the cathedral and a relatively smaller streamwise velocity at the leading edge of the upstream canyon obstacle, respectively. Similar patterns in the streamwise and vertical components within the canyon are observed in both configurations, while those in the 1-block configuration show a slightly larger magnitude and spatial extent. The standard deviation of the vertical velocity component shows

extremely distinct patterns since the regions with maximum magnitudes are at different canyon corners at the pedestrian level.

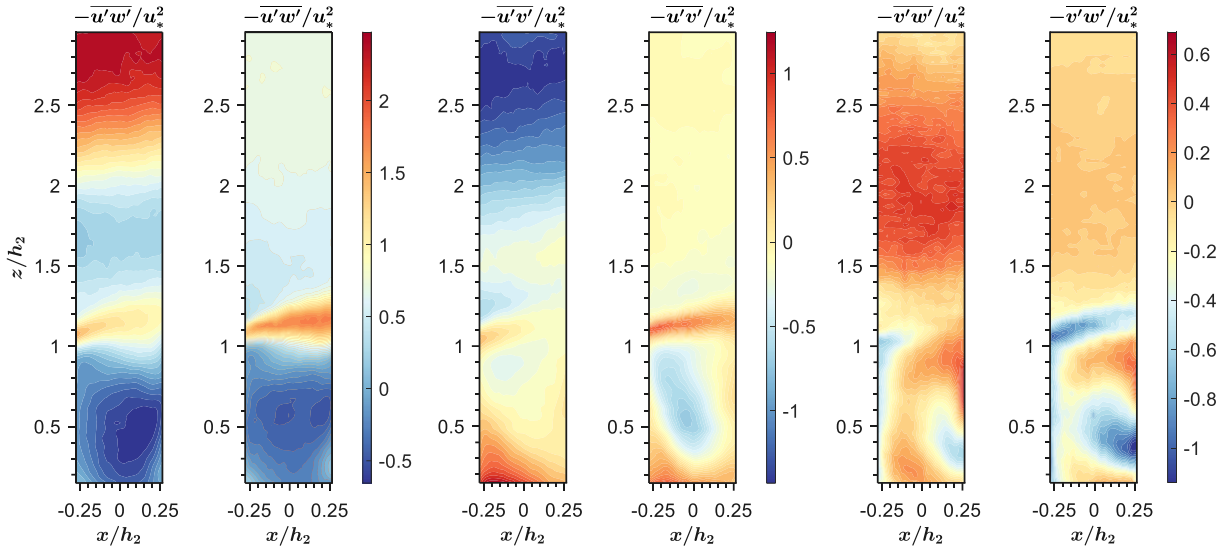

Fig 4. Comparison of contours of Reynolds stresses (Left: cathedral; Right: 1-block)

Reynolds stresses (Fig 4.), interpreted as momentum fluxes, could bring insights into turbulent kinetic energy (TKE) production. Within the shear layer caused by the upstream canyon leading-edge, $-\overline{u'w'}$ and $-\overline{u'v'}$ are positive but the $-\overline{v'w'}$ is negative. The $-\overline{u'w'}$ between $z/h_2 = 2$ and 3, and $-\overline{v'w'}$ between $z/h_2 = 1.5$ and 2.5 over the canyon in the cathedral configuration show a large positive value, but the $-\overline{u'v'}$ within the same region show a negative value. A large positive $-\overline{u'v'}$ is observed at the upstream lower corner of the canyon whilst there is an elliptical region of negative $-\overline{u'v'}$ immediately below the shear layer which penetrates deep into the canyon. The negative $-\overline{v'w'}$ extends from the shear layer along the upstream wall and also has a local minimum at the downstream wall between $z/h_2 =$ 0.2 and 0.6.

Higher-order moments of velocities such as skewness (Fig 5.) and flatness (Fig 6.) help characterize the shape of the probability density function (PDF). The value of a non-zero skewness indicates whether the probability of the existence of larger velocity excursions in one direction is greater than in the others. A larger flatness shows whether the occurrence of larger excursions from mean values is more frequent.

The streamwise skewness S_u is highly positive in the shear layer for both configurations. Positive S_u is observed in the wake-affected boundary layer in the cathedral configuration while in the 1-block configuration, the S_u shows a negative region immediately above the shear layer and stays negative in the overlying boundary layer. Within the canyon, the major part of the downstream near-wall region is positively skewed and the upstream near-wall region is negatively skewed. Similar patterns occur between the cathedral and 1-block configurations for the skewnesses of the vertical and spanwise components, although a large difference is the positive vertical skewness in the boundary layer over the canyon downstream of the block. It is worth noting that there is a strongly positive elliptical area in the canyon for the skewness of the spanwise velocity component near the downstream wall. The positive areas suggest that the PDFs of velocity in a certain direction at these

locations have a peak value that is smaller than the mean value while the tail is larger, and they show that the dominant modes are slower than the mean wind speeds in this corresponding direction.

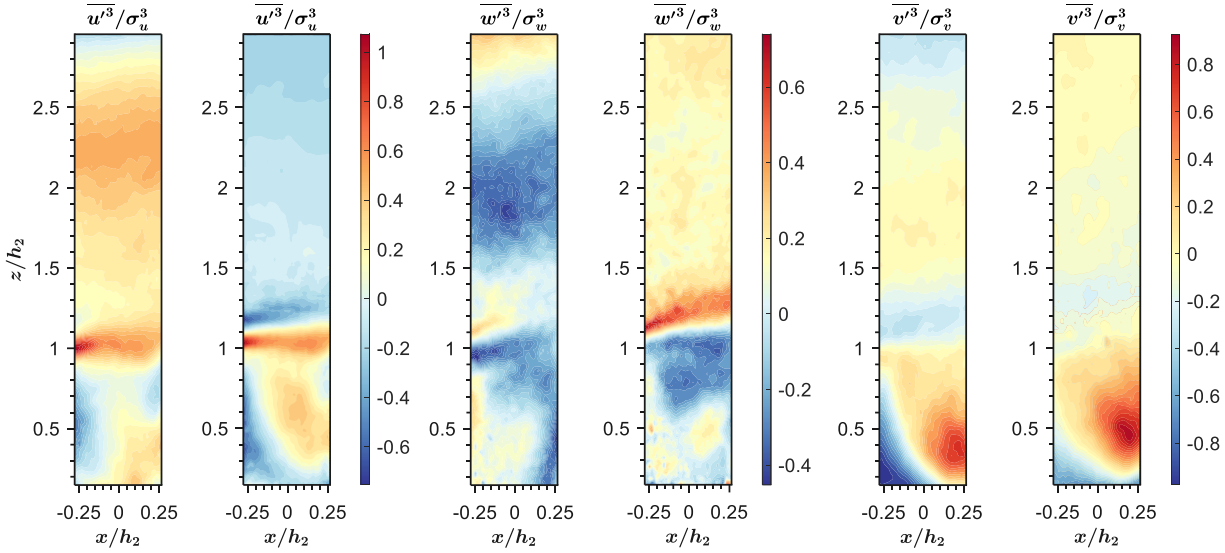

Fig 5. Comparison of contours of velocity skewness (Left: cathedral; Right: 1-block)

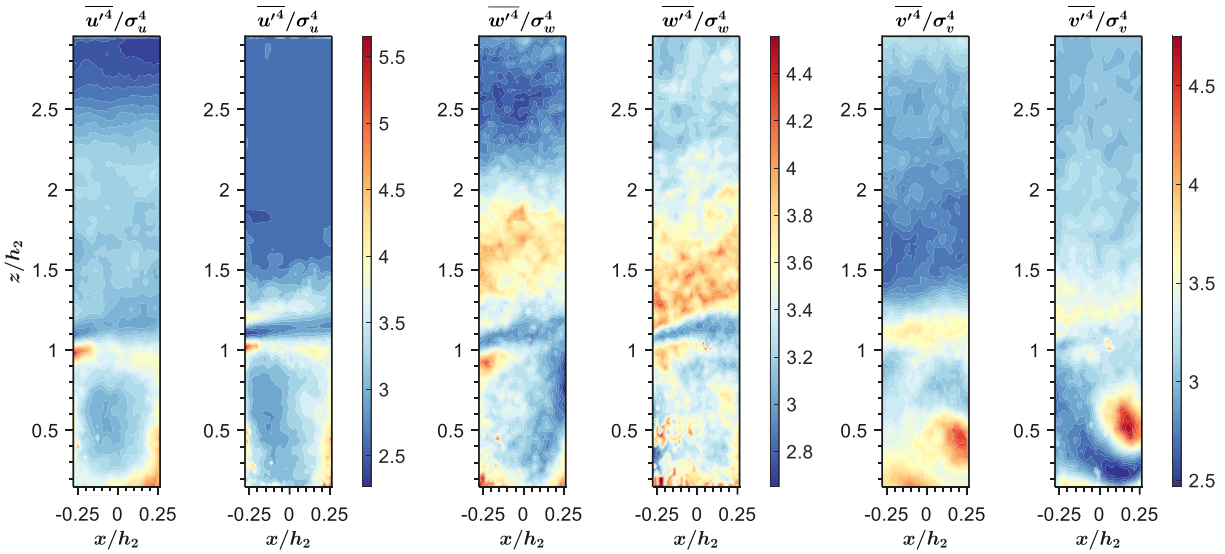

Fig 6. Comparison of contours of velocity flatness (Left: cathedral; Right: 1-block)

Differences in the velocity flatness (kurtosis) between the two configurations are not apparent. The upper limit of the shear layer shows a strongly flattening effect in the streamwise direction. The region between z/h_2 = 1.2 to 2 has a much more elevated peak in the vertical PDF than a normal distribution. A more peaked region is found at the bottom of the street canyon for the cathedral model than the 1-block model for the spanwise flatness, but a similar high-value core appears near the downstream wall.

Conclusion

In the present work, the flow within and above a street canyon immersed within a morphological model with or without an upstream tall building was investigated through the analysis of the main

one-point statistics, and the following conclusions were drawn. The wake caused by the upstream cathedral has a strong effect on the turbulence statistics in comparison to the 1-block situation. The presence of the cathedral decreases the $-\overline{u'w'}$, σ_u, σ_w and S_w within the shear layer, in comparison to the 1-block configuration, and this results in weaker vertical exchanges at the roof level. Strong spanwise velocities were found at the pedestrian level at the upstream corner of the canyon in both configurations, which could be explained by the heterogeneity caused by the intersections along the canyon. However, the spanwise velocity in the cathedral configuration smaller while being more turbulent than in the 1-block configuration. The influence of the upstream tall building and the coupling between the flow within the canyon and the overlying flow will be investigated in future work.

Reference

Barlow, J., Best, M., Bohnenstengel, S. I., Clark, P., Grimmond, S., Lean, H., Christen, A., Emeis, S., Haeffelin, M., Harman, I. N., Lemonsu, A., Martilli, A., Pardyjak, E., Rotach, M. W., Ballard, S., Boutle, I., Brown, A., Cai, X., Carpentieri, M., … Zhong, J. (2017). Developing a research strategy to better understand, observe, and simulate urban atmospheric processes at Kilometer to Subkilometer Scales. *Bulletin of the American Meteorological Society*, *98*(10), ES261–ES264. https://doi.org/10.1175/BAMS-D-17-0106.1

Basley, J., Perret, L., & Mathis, R. (2019). Structure of high Reynolds number boundary layers over cube canopies. *Journal of Fluid Mechanics*, *870*, 460–491. https://doi.org/10.1017/jfm.2019.274

Berkowicz, R. (2000). OSPM - A Parameterised Street Pollution Model. *Environmental Monitoring and Assessment*, *65*(1–2), 323–331. https://doi.org/10.1007/978-94-010-0932-4_35

Berkowicz, R., Ketzel, M., Vachon, G., Louka, P., Rosant, J.-M., Mestayer, P. G., & Sini, J.-F. (2002). Examination of traffic pollution distribution in a street canyon using the Nantes'99 experimental data and comparison with model results. *Urban Air Quality — Recent Advances*, 311–324. https://doi.org/10.1007/978-94-010-0312-4_22

Blackman, K., Perret, L., & Savory, E. (2015). Effect of upstream flow regime on street canyon flow mean turbulence statistics. *Environmental Fluid Mechanics*, *15*(4), 823–849. https://doi.org/10.1007/s10652-014-9386-8

Blackman, K., Perret, L., & Savory, E. (2018). Effects of the upstream-flow regime and canyon aspect ratio on non-linear interactions between a street-canyon flow and the overlying boundary layer. *Boundary-Layer Meteorology*, *169*(3), 537–558. https://doi.org/10.1007/s10546-018-0378-y

Bottema, M. (1996). Roughness parameters over regular rough surfaces: Experimental requirements and model validation. *Journal of Wind Engineering and Industrial Aerodynamics*, *64*(2–3), 249–265. https://doi.org/10.1016/S0167-6105(96)00062-1

Brixey, L. A., Heist, D. K., Richmond-Bryant, J., Bowker, G. E., Perry, S. G., & Wiener, R. W. (2009). The effect of a tall tower on flow and dispersion through a model urban neighborhood: Part 2. Pollutant dispersion. *Journal of Environmental Monitoring*, *11*(12), 2171–2179. https://doi.org/10.1039/b907137g

Castro, I. P., Segalini, A., & Alfredsson, P. H. (2013). Outer-layer turbulence intensities in smooth- and rough-wall boundary layers. *Journal of Fluid Mechanics*, *727*, 119–131. https://doi.org/10.1017/jfm.2013.252

Cheng, H., & Castro, I. P. (2002). Near wall flow over urban-like roughness. *Boundary-Layer Meteorology*, *104*(2), 229–259. https://doi.org/10.1023/A:1016060103448

Cheng, W. C., Liu, C. H., Ho, Y. K., Mo, Z., Wu, Z., Li, W., Chan, L. Y. L., Kwan, W. K., & Yau, H. T. (2021). Turbulent flows over real heterogeneous urban surfaces: Wind tunnel experiments and Reynolds-averaged Navier-Stokes simulations. *Building Simulation*, *14*(5), 1345–1358. https://doi.org/10.1007/s12273-020-0749-4

Choi, Y. K., Hwang, H. G., Lee, Y. M., & Lee, J. H. (2020). Effects of the roughness height in turbulent boundary layers over rod- and cuboid-roughened walls. *International Journal of Heat and Fluid Flow*, *85*(June), 108644. https://doi.org/10.1016/j.ijheatfluidflow.2020.108644

Eichhorn, J. (1996). Validation of a Microscale Pollution Dispersal Model. *Air Pollution Modeling and Its Application XI*, 539–547. https://doi.org/10.1007/978-1-4615-5841-5_56

Fuka, V., Xie, Z. T., Castro, I. P., Hayden, P., Carpentieri, M., & Robins, A. G. (2018). Scalar fluxes near a tall building in an aligned array of rectangular buildings. *Boundary-Layer Meteorology*, *167*(1), 53–76. https://doi.org/10.1007/s10546-017-0308-4

Goulart, E. V., Reis, N. C., Lavor, V. F., Castro, I. P., Santos, J. M., & Xie, Z. T. (2019). Local and non-local effects of building arrangements on pollutant fluxes within the urban canopy. *Building and Environment*, *147*(July 2018), 23–34. https://doi.org/10.1016/j.buildenv.2018.09.023

Grimmond, C. S. B., & Oke, T. R. (1999). Aerodynamic properties of urban areas derived from analysis of surface form. *Journal of Applied Meteorology*, *38*(9), 1262–1292. https://doi.org/10.1175/1520-0450(1999)038<1262:APOUAD>2.0.CO;2

Heist, D. K., Brixey, L. A., Richmond-Bryant, J., Bowker, G. E., Perry, S. G., & Wiener, R. W. (2009). The effect of a tall tower on flow and dispersion through a model urban neighborhood: Part 1. Flow characteristics. *Journal of Environmental Monitoring*, *11*(12), 2163–2170. https://doi.org/10.1039/b907135k

Hertwig, D., Gough, H. L., Grimmond, S., Barlow, J. F., Kent, C. W., Lin, W. E., Robins, A. G., & Hayden, P. (2019). Wake characteristics of tall buildings in a realistic urban canopy. *Boundary-Layer Meteorology*, *172*(2), 239–270. https://doi.org/10.1007/s10546-019-00450-7

Hertwig, D., Grimmond, S., Kotthaus, S., Vanderwel, C., Gough, H., Haeffelin, M., & Robins, A. (2021). Variability of physical meteorology in urban areas at different scales: Implications for air quality. *Faraday Discussions*, *226*, 149–172. https://doi.org/10.1039/d0fd00098a

Inagaki, A., & Kanda, M. (2008). Turbulent flow similarity over an array of cubes in near-neutrally stratified atmospheric flow. *Journal of Fluid Mechanics*, *615*, 101–120. https://doi.org/10.1017/S0022112008003765

Jaroslawski, T., Perret, L., Blackman, K., & Savory, E. (2019). The Spanwise Variation of Roof-Level Turbulence in a Street-Canyon Flow. *Boundary-Layer Meteorology*, *170*(3), 373–394. https://doi.org/10.1007/s10546-018-0405-z

Kastner-Klein, P., Berkowicz, R., & Britter, R. (2004). The influence of street architecture on flow and dispersion in street canyons. *Meteorology and Atmospheric Physics*, *87*(1–3), 121–131. https://doi.org/10.1007/s00703-003-0065-4

Kastner-Klein, Petra, & Rotach, M. W. (2004). Mean flow and turbulence characteristics in an urban roughness sublayer. *Boundary-Layer Meteorology*, *111*(1), 55–84. https://doi.org/10.1023/B:BOUN.0000010994.32240.b1

Lim, H. D., Hertwig, D., Grylls, T., Gough, H., Reeuwijk, M. van, Grimmond, S., & Vanderwel, C. (2022). Pollutant dispersion by tall buildings: laboratory experiments and Large-Eddy Simulation. *Experiments in Fluids*, *63*(6), 1–20. https://doi.org/10.1007/s00348-022-03439-0

Louka, P., Vachon, G., Sini, J.-F., Mestayer, P. G., & Rosant, J.-M. (2002). Thermal Effects on the Airflow in a Street Canyon – Nantes'99 Experimental Results and Model Simulations. *Water, Air and Soil Pollution*, *2*(5), 351–364. https://doi.org/10.1023/A:1021355906101

Mestayer, P. G., Vachon, G., & Rosant, J. (1999). The nantes '99 data base for model validation of air quality in streets. *8th Int. Conf. on Harmonisation within Atmospheric Dispersion Modelling for Regulatory Purposes*, 297–300.

Michioka, T., & Sato, A. (2012). Effect of incoming turbulent structure on pollutant removal from two-dimensional street canyon. *Boundary-Layer Meteorology*, *145*(3), 469–484. https://doi.org/10.1007/s10546-012-9733-6

Ng, E., Yuan, C., Chen, L., Ren, C., & Fung, J. C. H. (2011). Improving the wind environment in high-density cities by understanding urban morphology and surface roughness: A study in Hong Kong. *Landscape and Urban Planning*, *101*(1), 59–74. https://doi.org/10.1016/j.landurbplan.2011.01.004

Roh, S. C., & Park, S. O. (2003). Vortical flow over the free end surface of a finite circular cylinder mounted on a flat plate. *Experiments in Fluids*, *34*(1), 63–67. https://doi.org/10.1007/s00348-002-0532-6

Rotach, M. W., Vogt, R., Bernhofer, C., Batchvarova, E., Christen, A., Clappier, A., Feddersen, B., Gryning, S. E., Martucci, G., Mayer, H., Mitev, V., Oke, T. R., Parlow, E., Richner, H., Roth, M., Roulet, Y. A., Ruffieux, D., Salmond, J. A., Schatzmann, M., & Voogt, J. A. (2005). BUBBLE - An urban boundary layer meteorology project. *Theoretical and Applied Climatology*, *81*(3–4), 231–261. https://doi.org/10.1007/s00704-004-0117-9

Salizzoni, P., Marro, M., Soulhac, L., Grosjean, N., & Perkins, R. J. (2011). Turbulent transfer between street canyons and the overlying atmospheric boundary layer. *Boundary-Layer Meteorology*, *141*(3), 393–414. https://doi.org/10.1007/s10546-011-9641-1

Schultz, M., Leitl, B., & Schatzmann, M. (2007). How rough is rough ? Characterization of turbulent fluxes within and above an idealized urban roughness. *International Workshop on Physical Modelling of Flow and Dispersion Phenomena*, 69–74.

Sini, J. F., Anquetin, S., & Mestayer, P. G. (1996). Pollutant dispersion and thermal effects in urban street canyons. *Atmospheric Environment*, *30*(15), 2659–2677. https://doi.org/10.1016/1352-2310(95)00321-5

Squire, D. T., Hutchins, N., Schultz, M. P., & Klewicki, J. C. (2016). Erratum: Comparison of turbulent boundary layers over smooth and rough surfaces up to high Reynolds numbers (Journal of Fluid Mechanics (2016) 795 (210-240) DOI: 10.1017/jfm.2016.196). *Journal of Fluid Mechanics*, *797*, 917. https://doi.org/10.1017/jfm.2016.307

Takimoto, H., Inagaki, A., Kanda, M., Sato, A., & Michioka, T. (2013). Length-scale similarity of turbulent organized structures over surfaces with different roughness types. *Boundary-Layer Meteorology*, *147*(2), 217–236. https://doi.org/10.1007/s10546-012-9790-x

Tominaga, Y., & Shirzadi, M. (2021). Wind tunnel measurement of three-dimensional turbulent flow structures around a building group: Impact of high-rise buildings on pedestrian wind environment. In *Building and Environment*. https://doi.org/10.1016/j.buildenv.2021.108389

Vachon, G., Louka, P., Rosant, J.-M., Mestayer, P. G., & Sini, J.-F. (2002). Measurements of traffic-induced turbulence within a street canyon during the Nantes'99 experiment. *Urban Air Quality — Recent Advances*, *1986*, 127–140. https://doi.org/10.1007/978-94-010-0312-4_10

Yang, X. I. A., & Meneveau, C. (2016). Large eddy simulations and parameterisation of roughness element orientation and flow direction effects in rough wall boundary layers. *Journal of Turbulence*, *17*(11), 1072–1085. https://doi.org/10.1080/14685248.2016.1215604

Yuan, C., Ng, E., & Norford, L. K. (2014). Improving air quality in high-density cities by understanding the relationship between air pollutant dispersion and urban morphologies. *Building and Environment*, *71*(2), 245–258. https://doi.org/10.1016/j.buildenv.2013.10.008